A Novel Wind-Power Generating System Using Field Orientation Controlled Doubly-Excited Brushless Reluctance Machine

Longya Xu
Member, IEEE

Yifan Tang
Student Member, IEEE

The Ohio State University
Department of Electrical Engineering
2015 Neil Avenue
Columbus, Ohio 43210

Abstract- Variable speed operation of a wind turbine generator improves its energy capturing capability. Up to the present, the machines employed have been induction machines, conventional synchronous machines or DC machines. The major drawback of these machines is that a complicated arrangement of slip rings or commutators with brushes, and a full-rating power converter are required. Reliability and cost are major concerns for these systems. Slip power recovery system with a doubly-fed wound rotor induction machine uses a converter with substantially reduced power rating, yet the slip-ring and brushes are still required. A new variable speed constant frequency wind power generating system is proposed in this paper by using a doubly-excited brushless reluctance machine. A field orientation control method is proposed to track the optimal torque-speed profile of the wind turbine and to realize flexible reactive power control. The proposed wind power generating system has potentials of high efficiency, good flexibility and low cost.

INTRODUCTION

Wind power is one of the favorable clean energy sources that can partially solve the energy problem and environmental dilemma we are facing today. Wind power generators with ratings from 50 to 350 kilowatts are in use. The next technological breakthrough in the development of wind power generating will be penetration into areas with lower energy costs and poorer wind regimes. Variable speed wind power generating is considered an effective technology to enhance the penetration [1,2,3]. The improvement in energy capturing capability of a wind turbine generator by variable speed operation is, in effect, dual of the improvement in energy efficiency achieved by a variable speed drive when the fan type load is coupled to its shaft. An example of energy efficiency improvement for a wind-power generating system by variable speed operation is shown

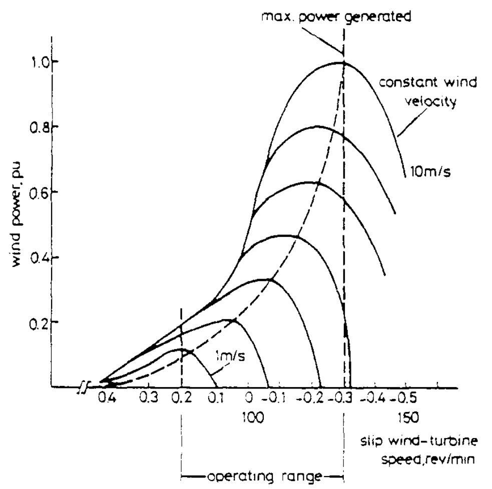

Fig. 1. Wind Turbine Power-speed Characteristics ([3])

in Fig. 1. As indicated, when the wind is at 10 m/s, the wind mill will capture maximum power if it runs at 130 rpm, while it only captures half of the maximum power if it runs at 100 rpm. A number of other important features are available which not only promise efficiency enhancement but also contribute greatly towards improved reliability. These features are rapid speed response to wind transients, damping of torsional modes, performance enhancement during electrical transients, and efficient system start-up and shut-down.

To link a variable speed wind turbine with the constant frequency power network, a variable speed constant frequency (VSCF) generating system is necessary. In high power ratings, major configurations of VSCF generating system include DC machine with line commutated inverter, synchronous machine with thyristor rectifier and inverter, doubly-excited induction machine with DC link rectifier and inverter, and doubly-excited induction machine with cycloconverter. Although these systems generally provide satisfactory performance, one important drawback is that a complicated arrangement of slip rings or commutators with brushes are required for the machines. This requirement degrades the performance of the system due to the reliability concerns of the slip rings and brushes and the associated high maintenance costs.

It has been suggested that the doubly fed brushless induction machine be used to solve the brush problem [4]. This machine is a self-cascaded induction machine which employs specially wound windings in the stator. These special windings are equivalent to two sets of stator windings with different pole pitches. The rotor is generally a squirrel cage type with dedicated pole pitch. While this machine has some attributes suitable for variable speed drives or generators, its efficiency is suffered from the short-circuit rotor currents.

A novel variable speed constant frequency generating system consisting of a bi-directional power converter and a Doubly Excited Brushless Reluctance Machine (DEBRM) is presented in this paper. This variable speed generating system is, in effect, dual of the variable speed drive system proposed in [5]. Since the rotor of the DEBRM does not carry currents in operation, it eliminates the slip rings, brushes and copper losses, resulting in a simpler and more reliable structure and higher efficiency.

A field orientation control method for the DEBRM is developed, based on a primary winding flux d-q model. Separate torque and reactive power control can be conveniently realized.

STRUCTURE AND OPERATION PRINCIPLES

A schematic description of the overall VSCF system using DEBRM is shown in Fig. 2. The stator of the DEBRM is wound in dual three phase winding arrangement. The rotor consists of simple saliency or axially laminated segments without windings, and the slip ring and brushes are not used. One important feature of the DEBRM is the pole number of the dual stator windings with respect to that of the rotor [6]. If one set of windings has pole number "$2p_1$" and the other "$2p_2$", the rotor pole pair number is constrained to "p_1+p_2". In VSCF operation, one of the two sets of stator windings, referred to as "primary windings" in this paper, is directly connected to the constant frequency power system and the other set of stator windings, or "secondary windings", is connected to the

0-7803-0634-1/92$03.00 ©IEEE

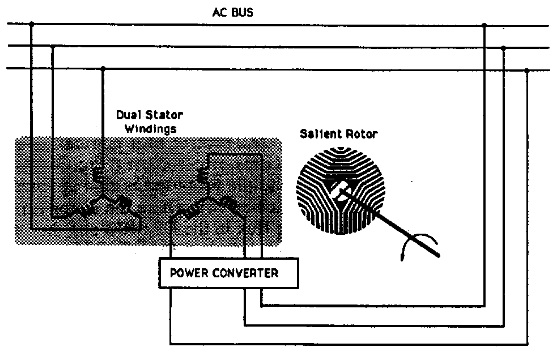

Fig. 2. Interconnection of the DEBRM Generator in Variable Speed Wind Power System

power system via a power converter. Induced speed voltage and electromechanical energy conversion occur when strong magnetic coupling between the two sets of stator windings is modulated by the saliency of the moving rotor. The primary frequency ω_1, secondary frequency ω_2 and the rotor speed ω_r satisfy the following constraint:

$$\omega_1 + \omega_2 = \omega_r (p_1 + p_2) \quad (1)$$

when the sequence of the three-phase currents in the two sets of stator windings are the same. Otherwise,

$$\omega_1 - \omega_2 = \omega_r (p_1 + p_2) \quad (2)$$

when the sequence of the three-phase currents in the two sets of stator windings are opposite to each other.

From (1) or (2), it can be seen that variable speed constant frequency operation of the DEBRM is realizable. For instance, given the primary frequency ω_1 to be constant, we can always control the the secondary frequency ω_2 to match the rotor speed variation so that Equations (1) or (2) is satisfied. Similar to the doubly-excited induction generator system, in the DEBRM system the power converter supplies slip-power to the secondary windings when the rotor speed is below the synchronous speed, and draws slip-power from the secondary windings when the rotor speed is above the synchronous speed.

The DEBRM has almost the same model and equivalent circuits as those of a wound-rotor doubly-fed induction machine [6]. The voltage equations of the DEBRM in the arbitrary rotating *d-q-n* reference frame are of the standard matrix form (motor convention),

$$\underline{v}_{dq1} = r_1 \underline{i}_{dq1} + \frac{d\underline{\lambda}_{dq1}}{dt} + \underline{\omega} \times \underline{\lambda}_{dq1} \quad (3)$$

where $\underline{\lambda}_{dq1} = \begin{pmatrix} \lambda_{d1} \\ \lambda_{q1} \\ \lambda_{n1} \end{pmatrix}$, $\underline{\omega} = \begin{pmatrix} 0 & -\omega & 0 \\ \omega & 0 & 0 \\ 0 & 0 & 0 \end{pmatrix}$,

$\underline{v}_{dq1} = \begin{pmatrix} v_{d1} \\ v_{q1} \\ v_{n1} \end{pmatrix}$, $\underline{i}_{dq1} = \begin{pmatrix} i_{d1} \\ i_{q1} \\ i_{n1} \end{pmatrix}$, $\underline{i}_{dq2} = \begin{pmatrix} i_{d2} \\ i_{q2} \\ i_{n2} \end{pmatrix}$,

and "x" represents vector cross product. ω is the rotating speed of the reference frame. The subscripts "1" and "2" denote the quantities associated with primary and secondary windings respectively. The primary winding flux linkages are related to the currents by

$$\underline{\lambda}_{dq1} = \underline{L}_1 \underline{i}_{dq1} + \underline{L}_m \underline{i}_{dq2} \quad (4)$$

where $\underline{L}_1 = \begin{pmatrix} L_1 & 0 & 0 \\ 0 & L_1 & 0 \\ 0 & 0 & L_1 \end{pmatrix}$, $\underline{L}_m = \begin{pmatrix} L_m & 0 & 0 \\ 0 & L_m & 0 \\ 0 & 0 & 0 \end{pmatrix}$.

The torque equation can be written as

$$T_e = \frac{3}{2}\frac{P}{2}(\lambda_{d1} i_{q2} - \lambda_{q1} i_{d2}) \quad (5)$$

where P denotes rotor pole number, i.e. $P = 2(p_1+p_2)$. The voltage equations of the secondary windings are not included assuming that the currents i_{q2} and i_{d2} or the voltages v_{q2} and v_{d2} are produced by a power converter.

Although the mathematical model of the DEBRM is very similar to that of an induction machine, the terminal constraints of the DEBRM in a VSCF generating system are very different from those of a cage induction motor in a variable speed drive system. For a cage induction motor, the input voltage at its rotor side is identically zero because of the short-circuit cage, and the input voltage at its stator side is conditioned to a proper magnitude, frequency and phase angle to achieve desired performance. While for the DEBRM in a VSCF generating system, as shown in Fig. 2, the magnitude and frequency of the primary voltage are constants defined by the power network and the secondary terminal receives fully controlled voltage or current from a power converter. As a result of the differences of the terminal constraints, variable speed operation of the DEBRM is substantially different from that of a singly-fed induction machine in many aspects:

1) Since the frequency and magnitude of the primary voltage are fixed, the levels of the primary winding flux linkage, secondary winding flux linkage and air-gap flux linkage will maintain approximately constant values.

2) Unlike a variable speed singly-excited induction motor in which the speed of the rotating flux is controllable and so is the slip of the rotor, the rotating field of the DEBRM has a constant speed. Therefore, to achieve variable speed operation, the only possibility is to change the slip frequency instead of changing both the primary frequency and the slip frequency. When the rotor speed is far away from the synchronous speed, the slip frequency of the secondary circuit is substantial.

3) Speed and torque are controllable through the power converter linked to the secondary circuit. However, energy circulation by slip power recovery is inevitable for higher efficiency operation of the system.

FIELD ORIENTATION CONTROL OF DEBRM

In a wind power generating system, control schemes for the DEBRM are expected to achieve the following objectives: 1) The generator is required to track a prescribed torque-speed curve for maximum wind power capturing; 2) The output voltage frequency has to be constant; 3) Flexible reactive power control capability is achievable. Taking the operational differences between the DEBRM and a singly-fed induction machine into consideration, we have developed a field orientation control (FOC) strategy to realize the control objectives. The FOC of the DEBRM is based on the primary winding flux model.

In the primary winding flux model, the reference frame is rotating synchronously with respect to the primary winding flux, with the reference frame d-axis instantaneously overlaps the axis of the primary winding flux. In short, $\omega = \omega_1$ and $\lambda_{q1} = 0$. For such a reference frame selection, the system equations are reduced to:

$$v_{d1} = r_1 i_{d1} + \frac{d\lambda_{d1}}{dt} \quad (6)$$

$$v_{q1} = r_1 i_{q1} + \omega_1 \lambda_{d1} \tag{7}$$

$$\lambda_{d1} = L_1 i_{d1} + L_m i_{d2} \tag{8}$$

$$\lambda_{q1} = 0 = L_1 i_{q1} + L_m i_{q2} \tag{9}$$

Furthermore, if the primary voltage magnitude v_m is assumed, then

$$v_{q1}^2 + v_{d1}^2 = v_m^2 \tag{10}$$

Since the d-axis of the reference frame is the instant axis of the primary winding flux, the phase angle of the primary voltage is generally not a constant in the reference frame, although its frequency and magnitude are constants constrained by the power system. The electromagnetic torque is now

$$T_e = \frac{3}{2}\frac{P}{2} \lambda_{d1} i_{q2} \tag{11}$$

A torque production diagram derived from (6) through (11) is shown in Fig. 3(a). The torque production diagram of a singly excited induction machine is shown in Fig. 3(b) for comparison.

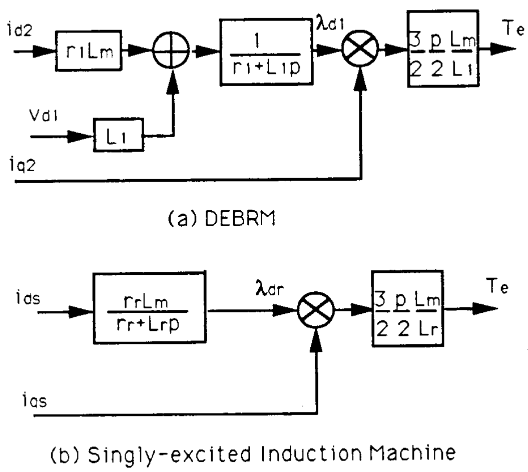

Fig. 3. Torque Production for Field Orientation Control

As discussed previously, the level of the primary winding flux remains approximately unchanged, restricted by the constant magnitude and frequency of the primary voltage. Therefore, the torque control of the DEBRM can be most conveniently achieved by controlling the secondary current component orthogonal to the primary winding flux.

The reactive power at the terminal of the primary winding, again in motor convention, can be expressed as

$$Q_1 = \frac{3}{2}(v_{q1} i_{d1} - v_{d1} i_{q1}) \tag{12}$$

or, from (6) and (7), with the primary winding flux remains unchanged,

$$Q_1 = \frac{3}{2}\omega_1 \lambda_{d1} i_{d1} \tag{13}$$

As indicated by (8), i_{d1} can be controlled by i_{d2}. Therefore, from (13), d-axis component of the secondary current, i_{d2}, can be controlled to regulate the reactive power.

As can be seen from (11) and (13), control of torque via i_{q2} and control of reactive power via i_{d2} are essentially decoupled, thus a decoupler is not needed to implement field orientation control. In addition, flux control is generally unnecessary since it maintains a constant level, while control of the reactive power becomes possible.

The primary winding field oriented control of the DEBRM is analogous to the rotor field oriented control of a popular singly-excited induction motor, as is obvious by comparing Fig. 3(a) with Fig. 3(b). Note that the FOC principle proposed is also applicable to a doubly-excited induction machine [8], where the stator flux is analogous to the primary winding flux in the DEBRM and the rotor circuit is analogous to the secondary circuit in the DEBRM.

FOC IMPLEMENTATION AND SIMULATION RESULTS

A. Implementation

Based on the principle discussed in the last section, Fig. 4 shows an implementation of the primary winding field orientation control strategy. A current-regulated pulse-width-modulation (CRPWM) voltage source inverter is used in the new VSCF generating system utilizing a DEBRM. To interface the secondary stator windings to the power network, another PWM voltage source inverter (VSI) is used. This PWM VSI can maintain a constant voltage at the DC side, therefore the size of the DC link filter can be reduced; also it can improve interface performance (power factor and harmonic distortion factor) at the AC side. The ability of bi-directional power flow is necessary for the generating system to achieve both sub-synchronous and super-synchronous speed operation. The kVA rating of the power converters is only a portion of the full rating of the DEBRM, depending on the machine speed range and normal power factor requirement.

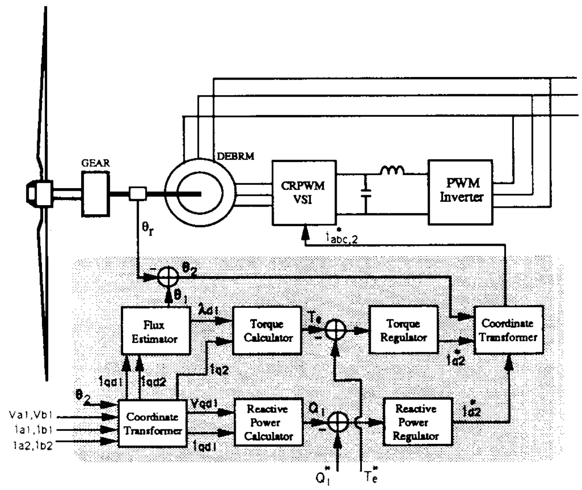

Fig. 4. Field Orientation Control Implementation

In order to control the dynamic torque, the instantaneous position and magnitude of the primary winding flux is made available through a flux estimator. A secondary current vector is injected orthogonally to the primary winding field, proportional to the command of the torque. Flexible reactive power control is achieved by controlling the primary current component in the d-axis of the primary winding field. In addition, the second PWM converter can provide reactive power to the secondary circuit.

B. Steady-state Characteristics of DEBRM

As discussed in the previous section, using the primary winding flux model, electromagnetic torque control is decoupled from reactive power control. This and other steady-state characteristics of the DEBRM are simulated in this section, based on the formulations derived in *Appendix*. A 50hp DEBRM with parameters similar to a typical doubly-excited induction machine is used in the simulation.

Fig. 5 shows the torque T_e, the reactive power Q_1, the primary winding flux λ_{d1}, and the primary voltages v_{q1} and v_{d1} controlled by i_{q2} or i_{d2} while i_{d2} or i_{q2} is fixed. It is shown that T_e and Q_1 are independently controlled by i_{q2} and i_{d2} respectively. Fig. 5 (b) shows that λ_{d1} is nearly unaffected by changing i_{q2} or i_{d2} and Fig. 5 (d) shows that v_{d1} is negligibly small.

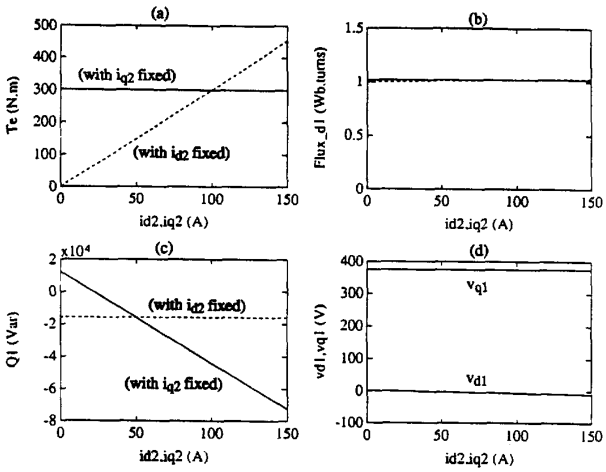

Fig. 5. Decoupling of T_e and Q_1

Fig. 6 shows the steady-state characteristics of the DEBRM generating system in a speed range covering both sub-synchronous and super-synchronous speeds. Wind-turbine characteristic of Fig. 1 is assumed, from which optimal generated power and wind-turbine torque corresponding to each speed can be determined. It is seen that the electromagnetic torque T_e is controlled by i_{q2} to track the optimal torque-speed profile of the wind-turbine, and the reactive power Q_1 is controlled by i_{d2}, as indicated in Fig. 6 (b).

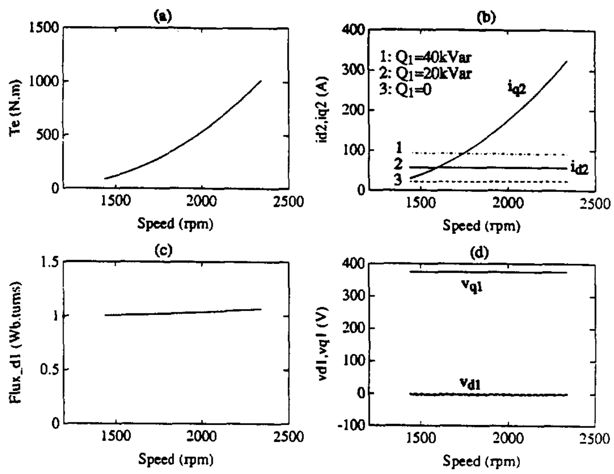

Fig. 6. Steady-state Characteristics of DEBRM

C. Dynamic Responses

Fig. 7 shows speed-tracking characteristics of the field orientation controlled DEBRM when the wind speed increases linearly in 4 seconds. As shown in Fig. 7 (a), through appropriate gearing between the wind-turbine and the generator shaft, the corresponding speed reference covers both sub-synchronous and super-synchronous speeds. Again, assume a wind-turbine characteristic of Fig. 1. In this particular simulation, electromagetic torque is controlled to have two step changes, one at the instant speed reaches synchronous speed and the other at the instant speed reaches steady-state. As can be seen from Fig. 7 (e), currents in the secondary windings are controlled by the power converter to have correct slip frequencies.

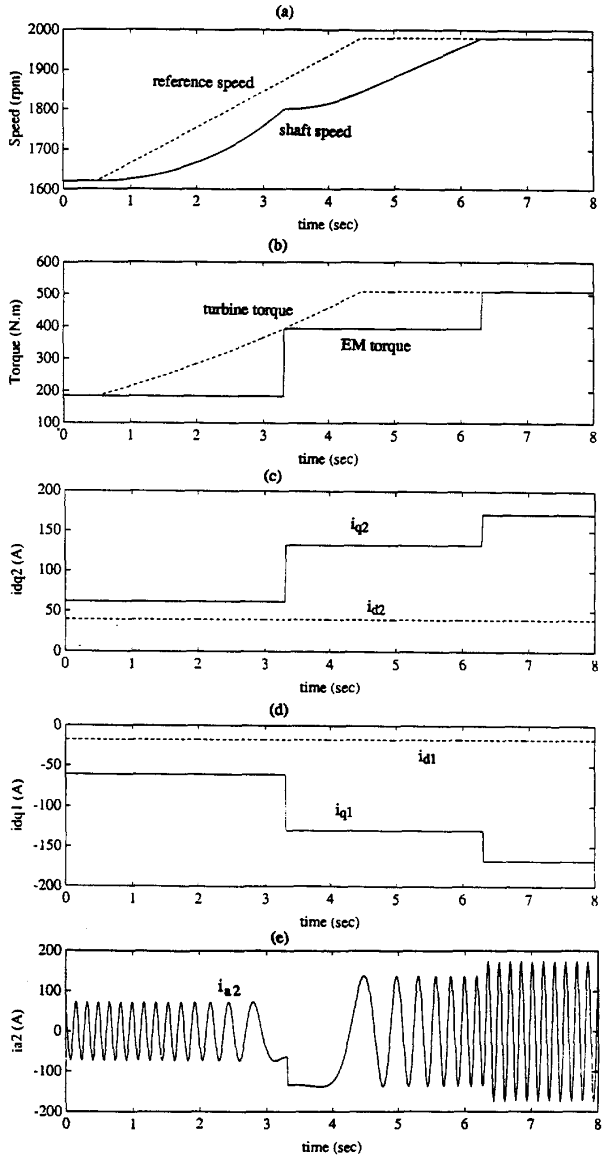

Fig. 7. Speed-tracking of Field Orientation Controlled DEBRM

Fig. 8 (a) shows the controlling of electromagnetic torque T_e. Fig. 8 (b) shows Q_1 with the reactive power command unchanged. Fig. 8 (c) shows corresponding i_{q2} and i_{d2}. Primary winding phase current and voltage i_{a1} and v_{a1} are shown in Fig. 8 (d). Fig. 9 shows the quantities of interest while reactive power command is changed and torque command is unchanged.

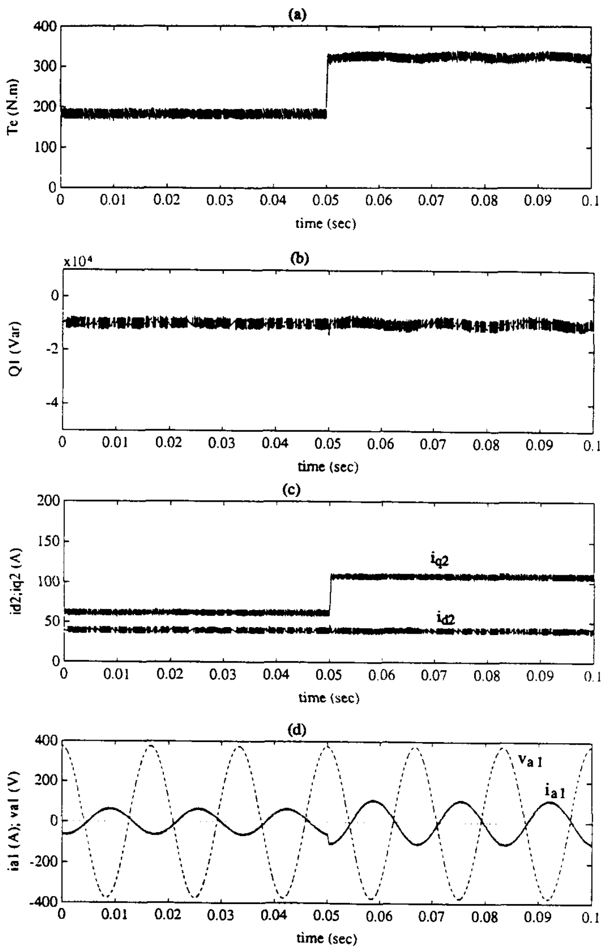

Fig. 8. Control of Electromagnetic Torque

CONCLUSIONS

A new variable speed constant frequency wind-power generating system is proposed in this paper. The core component of this system is the DEBRM. A field orientation control method is developed. Steady state and dynamic simulation shows feasibility of the generating system and validity of the high-performance control strategy.

The advantages and features of the proposed wind-power generating system can be summarized in the following:

i) High efficiency. This is a result of the improved energy capturing capability by variable speed operation of the generator to track the optimal torque-speed profile of the wind-turbine. In addition, there are no copper and brush losses on the rotor since no rotor windings and brushes are used.

ii) Enhanced reliability and reduced costs. The enhanced reliability is achieved by eliminating rotor windings, slip rings and brushes in the DEBRM. Cost reduction is achieved by reducing construction and maintenance costs, and by reducing the required kVA rating of the converter.

iii) Improved controllability and flexibility. With the high performance field orientation control strategy, the bi-directional power converter provides convenient control over the active and reactive power flow of the system, which makes the system more flexible for optimum operation.

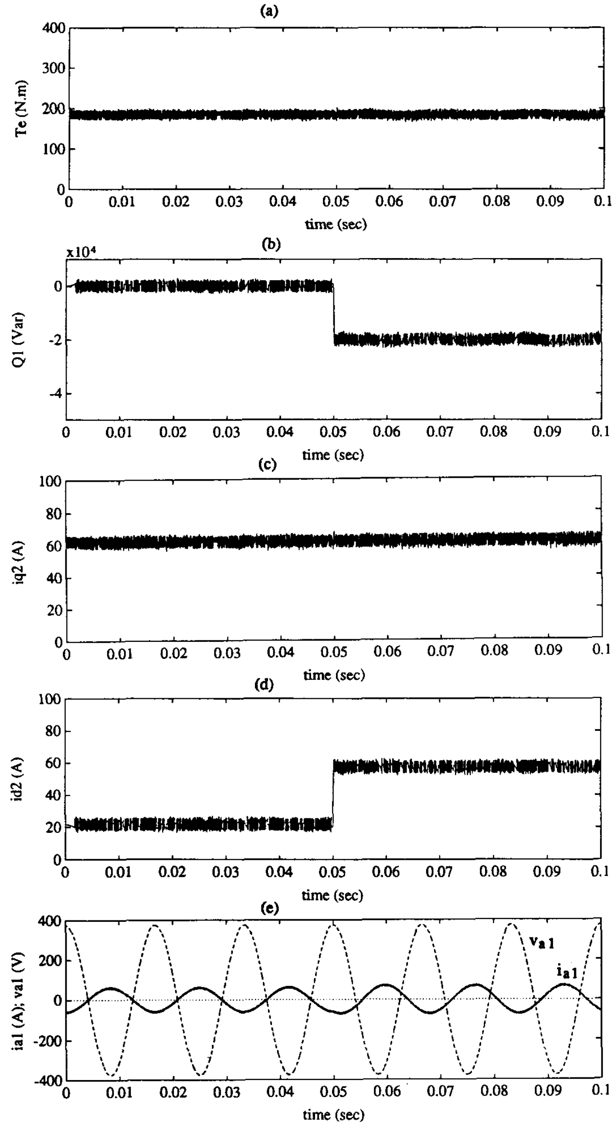

Fig. 9. Control of Reactive Power

ACKNOWLEDGMENT

The work in this paper is supported by a Research Initiation Grant from the National Science Foundation and a Seed Grant from The Ohio State University.

REFERENCES

1) F. R. Goodman, Jr., "Price Targets for Wind Turbines in Utility Applications", Windpower '85, San Francisco, CA, Aug. 27-30, 1985

2) T. A. Lipo, "Variable Speed Generator Technology Options for Wind Turbine Generators", DOE/NASA Workshop on

Horizontal-Axis Wind Turbine Technology, Cleveland, Ohio, May 8-10, 1984.

3) P. G. Holmes, and N. A. Elsonbaty, "Cycloconvertor-Excited Divided-Winding Doubly-Fed Machine as Wind -Power Convertor", IEE Proceedings, Vol. 131, Pt. B, No. 2, March 1984, pp. 61-69

4) R. Li, A. Wallace and R. Spee, "Dynamic Simulation of Brushless Doubly-Fed Machines", IEEE PES 1991 Winter Meeting, New York, New York, Feb. 3-7, 1991

5) L. Xu, F. Liang and T. A. Lipo, "Analysis of a New Variable Speed Doubly Excited Reluctance Motor", Electric Machines and Power System, Vol. 19. No. 2, March 1991, pp. 125-138.

6) L. Xu, F. Liang, and T. A. Lipo, "Transient Model of a Doubly Excited Reluctance Motor", IEEE Transaction on Energy Conversion, Vol. 6, No. 1, March 1991, pp. 126-133.

7) D. W. Novotny and R. D. Lorenz, (edited) "Introduction to Field Orientation and High Performance AC Drives", Second Edition, IEEE Industry Application Society Tutorial Course, 1986

8) Y. Tang, L. Xu, "Stator Field Oriented Control of Doubly-Excited Induction Machine in Wind Power Generating System", 35th Midwest Symposium on Circuits and Systems, Washington, DC, August 9-12, 1992

9) P. C. Krause, "Analysis of Electric Machinery", McGraw Hill, 1986

Appendix DEBRM Steady-state Characteristics

If the d-q reference frame is chosen to have its d-axis instantaneously overlap the axis of the primary winding flux, the steady-state model of the DEBRM can be obtained by setting time derivative terms to zero in (6) through (12),

$$v_{d1} = r_1 i_{d1} \qquad \text{A-1}$$

$$v_{q1} = r_1 i_{q1} + \omega_1 \lambda_{d1} \qquad \text{A-2}$$

$$\lambda_{d1} = L_1 i_{d1} + L_m i_{d2} \qquad \text{A-3}$$

$$\lambda_{q1} = 0 = L_1 i_{q1} + L_m i_{q2} \qquad \text{A-4}$$

$$v_{q1}^2 + v_{d1}^2 = v_m^2 \qquad \text{A-5}$$

$$T_e = \frac{3}{2}\frac{P}{2}\lambda_{d1} i_{q2} \qquad \text{A-6}$$

$$Q_1 = \frac{3}{2}\omega_1 \lambda_{d1} i_{d1} \qquad \text{A-7}$$

To study the effects of changing i_{q2} and i_{d2} towards the primary currents, flux, the following equations can be derived. From A-3 and A-4, it follows that

$$i_{d1} = \frac{\lambda_{d1} - L_m i_{d2}}{L_1} \qquad \text{A-8}$$

$$i_{q1} = -\frac{L_m}{L_1} i_{q2} \,. \qquad \text{A-9}$$

Then from A-1, A-2 and A-3, it yields that

$$\left(\frac{r_1\lambda_{d1} - r_1 L_m i_{d2}}{L_1}\right)^2 + \left(-\frac{r_1 L_m}{L_1} i_{q2} + \omega_1 \lambda_{d1}\right)^2 = v_m^2 \qquad \text{A-10}$$

and that

$$\lambda_{d1} = \frac{2 r_1 L_m (r_1 i_{d2} + \omega_1 L_1 i_{q2}) + \sqrt{U}}{2 (r_1^2 + \omega_1^2 L_1^2)} \qquad \text{A-11}$$

where $U = 4 r_1^2 L_m^2 [v_m^2 - (r_1 i_{d2} - \omega_1 L_1 i_{q2})^2] + 4\omega_1^2 L_1^4 v_m^2$. Therefore, v_{d1}, v_{q1}, T_e and Q_1 can be obtained from A-1, A-2, A-6 and A-7 respectively.

Given the optimal torque-speed profile and reactive power command, the current commands i_{d2} and i_{q2} can be determined from the following derivation.

Let $T = \frac{2}{3}\frac{2}{P}\frac{L_1}{L_m} T_e$, then $\lambda_{d1} = \frac{T}{i_{q2}}$. From A-2 and A-4,

$$v_{q1} = r_1 i_{q1} - \omega_1 T \frac{L_m}{L_1 i_{q1}} \qquad \text{A-12}$$

From A-1, A-7 and A-12,

$$\frac{i_{d1}}{i_{q1}} = -\frac{2}{3}\frac{Q_1}{\omega_1 T}\frac{L_1}{L_m} \qquad \text{A-13}$$

From A-1, A-5 and A-12,

$$\left(r_1 i_{q1} - \omega_1 T \frac{L_m}{L_1 i_{q1}}\right)^2 + (r_1 i_{d1})^2 = v_m^2 \qquad \text{A-14}$$

From A-13 and A-14,

$$i_{q1} = -\sqrt{\frac{(v_m\omega_1 T L_m)^2 + 2(\omega_1 T L_m)^3 r_1/L_1 + \sqrt{W}}{2(r_1\omega_1 T L_m)^2 + 4(Q_1 r_1 L_1)^2/9}} \qquad \text{A-15}$$

where $W = v_m^4 + \frac{4\omega_1 T r_1 L_m v_m^2}{L_1} - \frac{16}{9} Q_1^2 r_1^2$.

Therefore, v_{q1}, v_{d1}, i_{d1}, i_{q2}, i_{d2}, λ_{d1} can be obtained from A-1, A-2, A-3, A-4, A-6 and A-13.

Using A-1 through A-15, the steady-state characteristics of the DEBRM are simulated and the results are shown in Figs. 4 and 5. It is evident from the simulation that: 1) $\lambda_{d1} \approx$ constant; 2) control of T_e and Q_1 by i_{q2} and i_{d2}, respectively, are decoupled; 3) optimal torque-speed profile can be followed. These results can also be observed from A-1 through A-7 or from its solutions given in this *Appendix*. Note that the primary winding resistance r_1 is very small resulting in that $v_{q1} \approx v_m$, $\lambda_{d1} \approx \frac{v_{q1}}{\omega_1}$. Thus,

$$T_e \approx \frac{3}{2}\frac{P}{2}\frac{v_m}{\omega_1} i_{q2} \qquad \text{A-16}$$

$$Q_1 \approx \frac{3}{2} v_m \frac{v_m - \omega_1 L_m i_{d2}}{\omega_1 L_1} \qquad \text{A-17}$$